JOURNAL OF GEOPHYSICAL RESEARCH, VOL 88, PAGES 493-499, JANUARY 1, 1983

A THRESHOLD EFFECT FOR SPACECRAFT CHARGING

Richard Christopher Olsen

Physics Department, The University of Alabama in Huntsville, Huntsville, Alabama 35899

Abstract. The existence of a threshold energy dependence is shown for the charging of geostationary spacecraft in eclipse. Applied Technology Satellite 6 and P78-2 (SCATHA) data show that plasma sheet fluxes must extend above 10 keV for these satellites to charge in eclipse. The existence of a threshold energy is significant because magnetospheric convection boundaries produce relatively sharp phase space boundaries, with electron fluxes falling rapidly above the energy associated with the local Alfven layer. The threshold effect is due to the shape of the normal secondary yield curve, in particular the high energy crossover, where the secondary yield drops below 1. A large portion of the ambient electron flux must exceed this energy for a negative current to exist.

Introduction

Eclipse charging events on geosynchronous satellites have been explained as the natural result of the balance between the currents due to ambient electrons, ambient ions, and the secondary fluxes generated by the ambient plasma [*DeForest,* 1972; *Garrett and DeForest*, 1979]. This paper presents the borderline case between no charging and large (kV) negative potentials, and the dependence of this transition on a threshold energy in the ambient plasma. The motivation for this study is the desire to understand the observation that in hundreds of eclipses observed by Applied Technology Satellites 5 and 6 and P78-2 (SCATHA), the observation of large negative potentials coincided with substantial fluxes over 10 keV. Also, in a few percent of the eclipse events observed on these satellites, relatively subtle changes in the environment produced substantial changes in the spacecraft potential. These changes in the environment were generally due to the convection of stable plasma populations past the satellite or motion of the spacecraft with respect to convection boundaries, rather than injections of hot plasma (substorms). (See *Kivelson et al.* [1979] for examples.) Of course, injections due to substorms can also provide the necessary increase in net current. In the following sections, the basic theory for eclipse charging is reviewed, followed by a statistical view of the charging dependence on an electron threshold energy, based on a survey of spectrograms. Next, an example of the changes in potential caused by small environment changes is shown, and then a recap of the statistical survey is shown, using a different criterion for the threshold energy.

Copyright 1983 by the American Geophysical Union.

Paper number 2A1406.
0148-0227/83/002A-1406$02.00

Charging Theory

The net current to a spacecraft in eclipse can be symbolized

$$I_{net} = q\left(F_i - F_e + F_{sec}\right)$$

$F_{i.}$ = ion flux integrated over the spacecraft surface;
F_e = electron flux integrated over the spacecraft surface;
F_{sec} = secondary fluxes due to primary impact.

In equilibrium, the net current to the spacecraft is zero.

Though secondary electron production due to ion impact is important, the major secondary yield term is that due to electron impact. Figure 1 shows a typical secondary yield curve, in this case for kapton, a common spacecraft material (adapted from *Leung et al.* [1981]). This curve shows the features typical of most materials. There is a peak yield, greater than 1, at energies of a few hundred electron volts. If most of the ambient flux is in this energy range, the outgoing secondary flux will exceed the incoming electron flux, and the spacecraft will charge positively until the outgoing fluxes are limited sufficiently to attain equilibrium (typically a few volts positive; see *Olsen* [1982]). Other common features are lower and upper crossover energies, where the yield equals 1. It is this characteristic of the yield curve which leads to the threshold energy effect. As the energy of the ambient plasma population increases, the net current due to electrons will eventually become negative, and the potential will then be determined by the balance of these fluxes and the ambient ion fluxes, at some negative potential. This characteristic of the secondary yield curve has been recognized, and indeed utilized, for laboratory measurements (*see Leung et al.* [1981], for example). *Rubin et al.* [1978] have used this characteristic of the secondary yield curve to show that the temperature of a Maxwellian distribution would determine whether or not charging would occur, and that there is a critical temperature for charging. The upper crossover energy of 1.0 keV shown here for kapton, and the maximum yield of 1.8, are relatively low compared to some of the other dielectrics encountered on spacecraft, such as teflon and mylar [*Willis and Skinner,* 1973], so it should be kept in mind that a spacecraft may require electron fluxes at well over 1 keV in order to charge. The dependence of surface potential on material properties has been explored by *Knott* [1972] and *Prokopenko and Laframboise* [1980], among others, using a few typical particle spectra. In the example which follows, the complementary case is presented of a constant material (the spacecraft) being exposed to a varying environment.

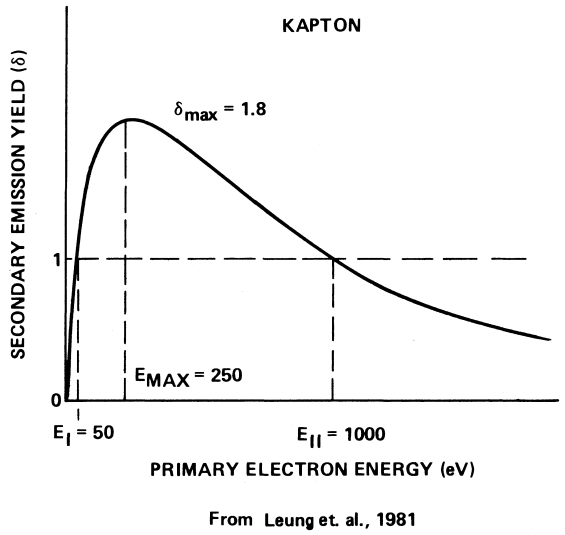

Fig. 1. Secondary electron yield due to electron impact for kapton. The number of secondary electrons produced by electron impact is plotted as a function of the energy of the primary electron [Leung et al., 1981].

Two relatively new terms are introduced below, i.e., transition energy and threshold energy. The first is the energy where the particle flux drops rapidly, or the energy where there is a distinct change in the distribution function. The term threshold energy is used to describe the transition energy associated with the beginning of the charging process.

Spacecraft and Instruments

Applied Technology Satellite 6 (ATS 6) was launched in 1974 into a geosynchronous orbit, where the three-axis-stabilized satellite con-ducted a variety of engineering and scientific experiments. The UCSD auroral particles experiment was an electrostatic analyzer (ESA) designed to measure ion and electron fluxes from 1 eV to 80 keV [*Mauk and Mcllwain,* 1975]. Two sets of electron and ion detectors sampled particle fluxes by rotating in orthogonal planes, providing good pitch angle and energy coverage in a few minutes. Energy resolutions (ΔE/E) is 20%, angular resolution 5° x 7°. The east-west (EW) detector assembly suffered a partial failure prior to the first eclipse season, limiting the energy range covered by this head. It still provides useful data within the energy range covered.

P78-2 (SCATHA) is an Air Force satellite designed to study spacecraft charging at and near geosynchronous orbit. It is in an equatorial, elliptical orbit, with perigee at 5.5 RE. and apogee at 7.5 RE. It was spin stabilized, with a spin period of about 57 s. A slightly modified version of the UCSD experiment from ATS 6 was flown on SCATHA.

Charging Survey

The initial motivation for this work was the observation that charging on ATS 6 and SCATHA required substantial fluxes over 10 keV. In this first view of the data, this observation is quantified. The survey was conducted by looking at spectrograms, as shown in Figure 2. The normal features of an eclipse charging event are found in these data from ATS 6 on October 4, 1974. This grey scale presentation of the particle fluxes uses black for zero flux, white for high fluxes, and grey for intermediate values. Plasma sheet electrons are visible throughout the 4-hour period shown here, extending from a few hundred eV to 10-20 keV. High photoelectron fluxes from 1 to 15 eV disappear during the eclipse (0530-0640 UT), with negative potentials evident from 0545 to 0640 UT in the ion data. Ambient ions reaching the spacecraft are accelerated by the spacecraft potential, and the absence of locally generated ions provides the characteristic charging signature of a large black region in the ion plot. There is no obvious differential charging signature in this data set [*Olsen, et* al. 1981; *Whipple,* 1976].

The transition energy is defined as the point where the electron fluxes drop from white to black (about 15 keV). This is partly an artifact of the logarithmic compression applied to the data before plotting, and inferences of boundaries in phase space cannot be safely done without creating and studying distribution functions. Since the count rate is proportional to E^2f, where f is the distribution function, the count rate naturally begins to drop above the normal peak at twice the temperature (for a

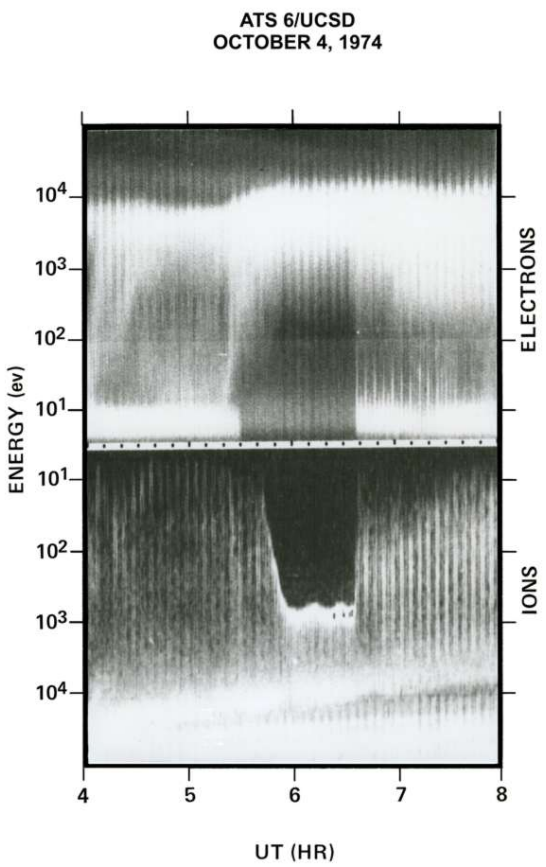

Fig. 2. ATS 6 energy-time spectrogram for October 4, 1974. Four hours of data from the NS detector show the ion and electron data around the eclipse event at local midnight. High fluxes are white, low fluxes are black. The energy scale is roughly logarithmic, going from 1 eV to 80 keV. Periodic vertical striping is due to detector rotation and pitch angle variations in the ambient plasma.

Maxwellian). This initial survey should be viewed with some caution, therefore, since the transition energy used in Figure 3 can be an artifact and not necessarily the convection boundary demonstrated in subsequent portions of this paper.

Figure 3 is a plot of observed eclipse potentials against transition energies, as determined from spectrograms. Again, the transition energy is the point where the electron count rate drops abruptly, typically from 10,000 Hz to a few hundred hertz. ATS 6 data from 40 eclipses in the fall of 1974 are combined with SCATHA data from 80 eclipses in 1979. Both spacecraft show a sharp increase in charging events when the electron flux goes above 15 keV. Once the threshold is crossed, however, the potentials reached by the spacecraft depend on other details of the ion and electron distribution functions, and no clear trend is found relating potential and threshold energy. In some of the largest ATS 6 and SCATHA charging events, the transition energy is over 80 keV.

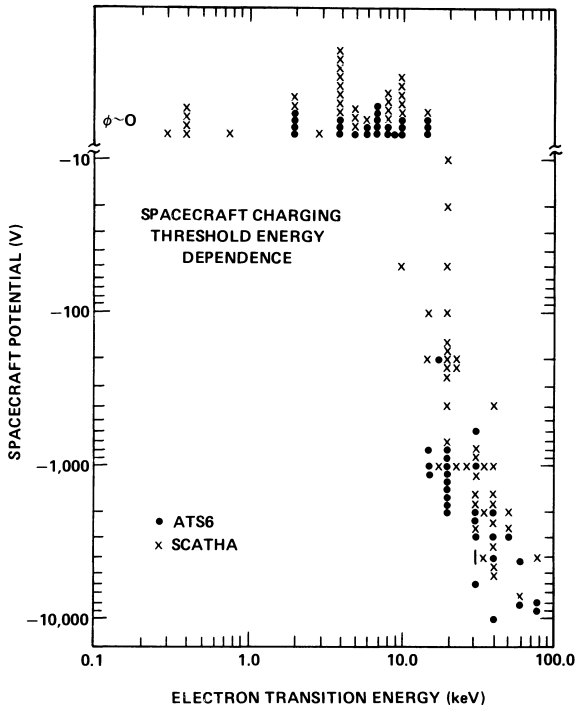

FIGURE 3. ATS 6 and SCATHA charging dependence on an electron threshold energy. The threshold energy used here is essentially the point where the electron count rate drops below the 1000 Hz point. This generally corresponds to the upper energy cutoff of the plasma sheet at the spacecraft location but can simply be an artifact of the detector response to keV particle distributions.

October 4, 1974

Figure 2 shows the event selected for more detailed analysis of the threshold energy and the relationship of this energy to variations in the electron distribution function and phase space boundaries. This is one of two events in the fall 1974 ATS 6 data set, where relatively small changes in the environment produced substantial changes in the spacecraft potential. Figure 4 shows the count rate for ions and electrons perpendicular to the magnetic field prior to and after the spacecraft charges. (Variations in the distribution function with pitch angle can be important, but in this case, the lack of recent magnetic activity has allowed the field-aligned portion of the electron population to be lost. The majority of the current is in the perpendicular fluxes.) The NS detector is rotating, sampling the pitch angle distribution of the plasma, while the EW detector is parked, measuring fluxes perpendicular to the magnetic field. The spacecraft was initially uncharged in eclipse (i.e., a few volts positive) and then, following a slight increase in electron energy at 0545 UT, began to charge negatively, reaching a maximum potential of.-700 V. This progression of events is visible in Figure 2 and will be expanded on in Figure 6.

Figures 4a and 4b show the ion and electron count rates from the NS and EW detectors at 0536 UT, when the spacecraft is near zero volts potential. The ion data show the absence of measurable potential, as was noted in the spectrogram. The minimum in ion flux at 20 keV is the 'deep proton minimum' as described by *Mcllwain* [1972]. This feature is the boundary between eastward and westward convecting ions, and the constancy of this feature in this example is evidence for a lack of substorm activity near the spacecraft. The electron data show a peak at about 7 keV and a rapid drop beginning at about 9 keV. The differences between the NS and EW detectors apparent in Figure 4b are due to pitch angle variations in the ambient plasma and differences in spiraltron efficiencies. Field-aligned data (not shown) reveal a normal electron loss cone. The 10 eV to 1 keV ion data show a source cone distribution.

Figure 4c and 4d show the ion and electron data at 0557 UT, when the spacecraft has reached a potential of -650 V. The peak in the ion flux between 600 and 700 eV shows the spacecraft potential signature. The energy of the proton minimum has dropped slightly during this period as a result of the spacecraft motion. These changes in the ion flux at high energy do not greatly affect the spacecraft current balance, and the ion data are ignored for the rest of the paper. The electron data show that the flux peak has moved up to 8 or 9 keV, with the drop in flux beginning at 12 keV.

Figure 5 shows the electron distribution functions for the NS detector data just shown, along with the result of fitting the 2- to 8-keV electron data with a Maxwellian. The 5-keV fits can be overlapped by shifting the distribution function by 650 eV, the change in spacecraft potential. This implies that other differences in the distribution functions are due to environmental changes.

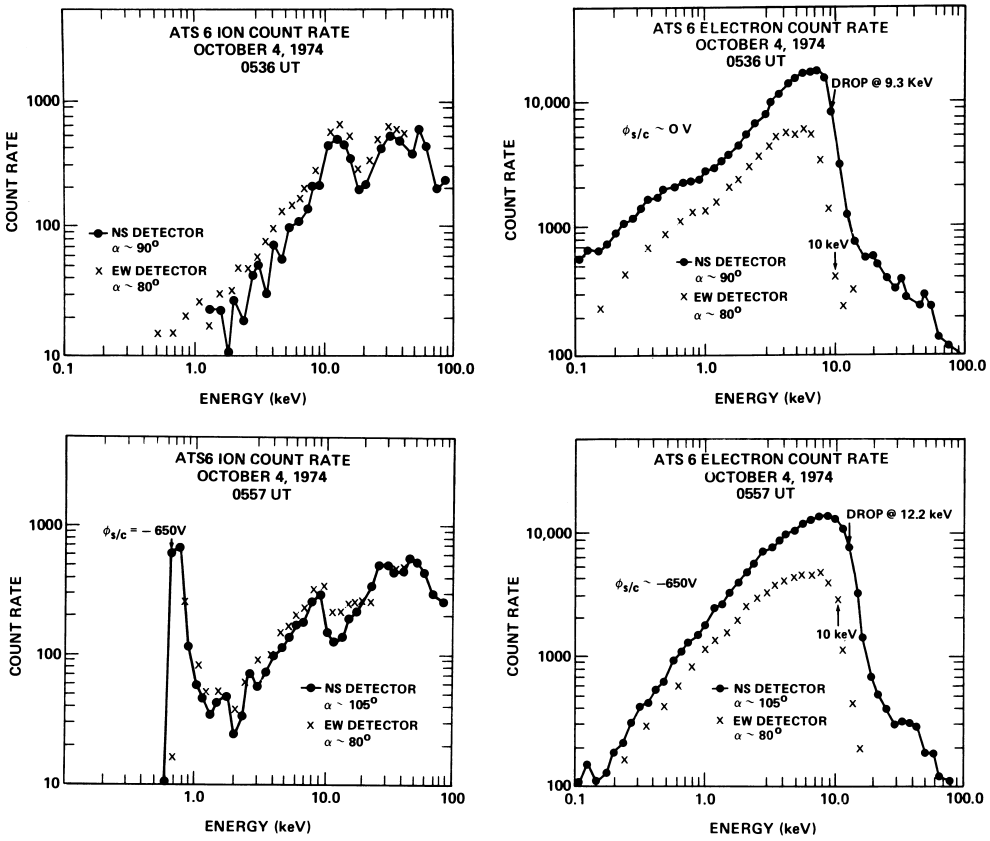

FIGURE 4. Electron and ion count rates from the NS and EW detectors on October 4, 1974. (a) Ion count rates at 0536 UT. One energy scan is plotted from the NS detector, while three scans have been averaged for the EW plot. Since the accumulation time is 4 s, count rates below 100 Hz are disturbed by statistical fluctuations. (b) Electron count rates at 0536 UT, one scan from each detector. NS fluxes are plotted as a solid line, EW fluxes as crosses. (c) Ion count rates at 0557 UT. One scan is plotted for the NS detector, two are averaged for the EW plot. (d) Electron count rates at 0557 UT, as in Figure 4c.

Also, the drop in the count rate at 9 keV at 0536 UT can be seen as the point where the observed distribution function drops below the nominal value it should have for a 5-keV Maxwellian. Similarly, the 0557 UT data begin to drop below the distribution function fit at 12-14 keV. This bend or break in the distribution function implies there is a phase space boundary at that energy. A phase space boundary is a boundary in velocity space for particle distribution functions. They are useful for separating plasmas with different origins, particularly if the populations are approximately Maxwellian, as electron distributions often are [*Whipple*, 1976; *Greenspan et al*. 1981]. In this case, the fact that the same temperature fit can be made for the 3- to 7-keV electrons implies that the nature of the plasma has not changed (i.e., it has not been heated). The changes in the distribution functions at 9 keV (0536 UT) and 12 keV (0557 UT) are apparently due to the Alfven boundary, the result of magnetospheric convection electric fields. The changes in the electron flux are therefore attributed to the crossing of the 10-keV Alfven boundary.

The changes in the spacecraft potential are therefore due to changes in the electron flux above 9 or 10 keV and not to the temperature of the distribution. Figure 6 shows this relation-ship over the time period when the potential was changing from 0 to -700 V, along with the electron fluxes at 6.5, 8.7, 10,0, and 11.5 keV. The lowest energy count rate shows little change over the time period and reflects the constancy of the plasma sheet population. The higher energy electron count rates show the changes attributed to the crossing of magnetospheric boundaries. The most dramatic change is in the 10-keV electron flux, which is initially excluded from the region of the spacecraft. Electrons of this energy associated with the 5-keV plasma population are on drift trajectories which are outside the initial spacecraft position. Changes in the spacecraft position (and perhaps the drift boundary) over the period of the eclipse bring the spacecraft into the 10- to 15-keV fluxes. The 8.7- and 10.0-keV fluxes both begin their climb between 0540 and 0545 UT, which is also the time associated with the beginning of the charging period. The spacecraft potential is deter-mined from the NS ion detector, and substantial fluxes are not measured in a charging peak until the potential has reached the -20 V point. This is largely a result of the lack of ambient low energy ions, and extrapolating the curve back to the -10 V point shows that the charging probably began at about 0540 UT, the time for the beginning of the increase in 9- to 10-keV electron fluxes.

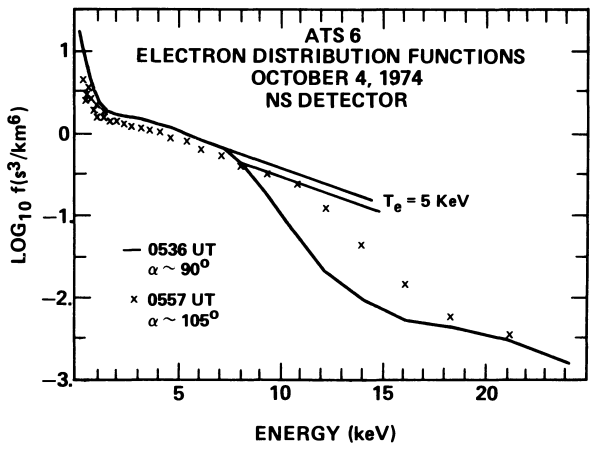

Fig. 5. Electron distribution functions for October 4, 1974, at 0536 and 0557 UT. The earlier time is plotted as a solid line, the latter as crosses. The parallel diagonal lines are the results of least squares fits between 3 and 7 keV. These fits gave electron temperatures of 5 keV and a density of about 1 cm^{-3}.

The change in the current to the spacecraft can be calculated from the observed changes in the distribution function. The observed change in the primary electron current density is about 15 pA/cm^2. Since the previously trapped electrons are now escaping and the spacecraft is nominally still near equilibrium (zero net current), this value is comparable to the in-crease in the current due to escaping secondary electrons. The increase in ion current is largely contained in the ion charging peak. The current density in the peak is only 1 pA/cm^2.

Statistical Look 2

Figure 7 shows a subset of the data from Figure 3, with the data points selected from those with a transition energy near 10 keV. In this plot, threshold energies are determined from distribution function plots for those days where it is clear that there is a distinct drop in the electron distribution function and therefore a boundary in phase space. The transition energy has been corrected for the spacecraft potential, so these- boundaries are those for the ambient plasma. It is clear that the crucial energy is about 15 keV for the cases shown here. The line noted D266 is a sequence of data for an ATS 6 event similar to the one just shown. Again, once the threshold has been passed, the correlation between threshold energy and potential is not a clear one.

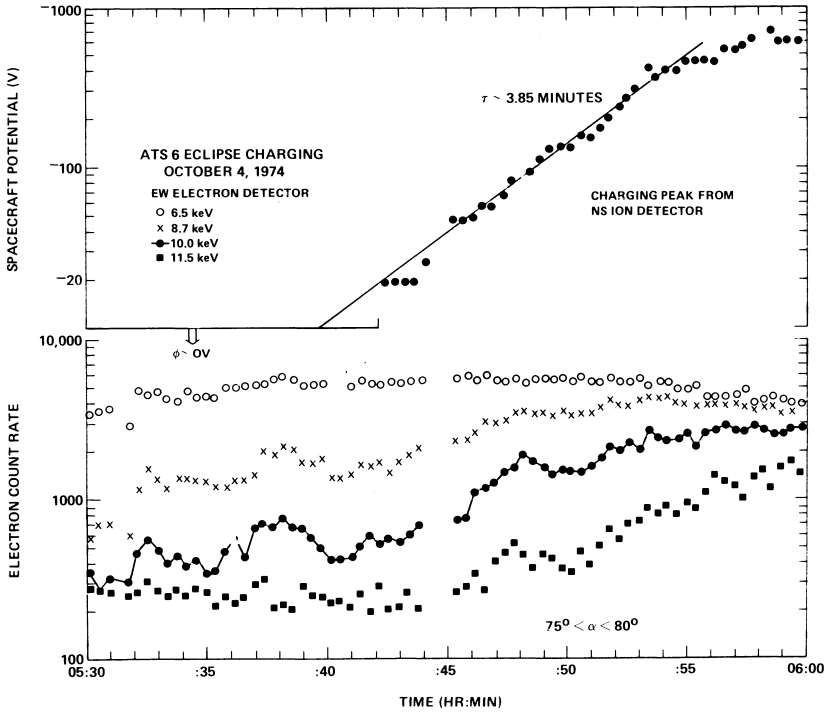

Fig. 6. Electron flux and spacecraft potential on October 4, 1974, in eclipse. Fluxes from the EW detector at 6.5, 8.7, 10.0, and 11.5 keV are plotted versus time here, along with the potential determined from the ion charging peak. The potentials between 0545 and 0555 UT were least square fitted for the 3.85 min time constant shown plotted through the potentials.

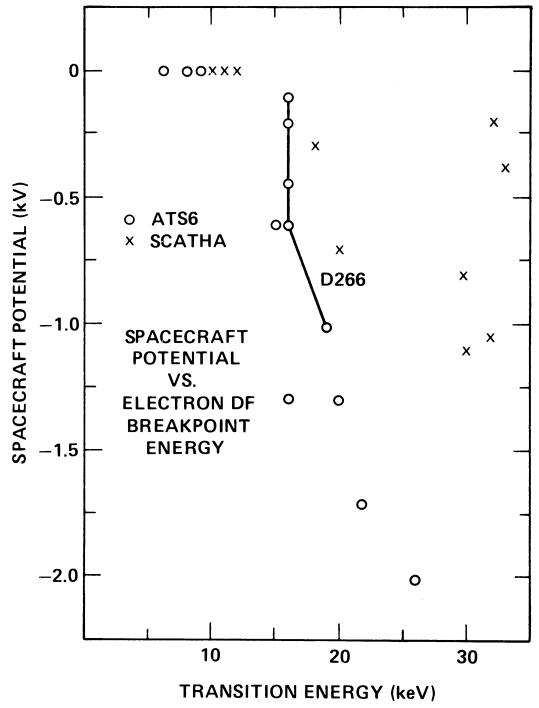

FIGURE 7. Spacecraft potentials are plotted against threshold energies determined from distribution functions.

Conclusions

The data from ATS 6 and SCATHA shown here have demonstrated the dependence of charging on the electron fluxes between 10 and 20 keV.

The transition from small positive potentials to large negative potentials has been shown to be associated with the movement of the spacecraft into plasma sheet regions `outside the 10-keV Alfven layer. Even in cases where the distribution function does not show characteristics associated with these spatial boundaries, it appears that the spacecraft does not charge unless there are substantial fluxes between 10 and 20 keV. For the UCSD detectors, this means the differential energy flux in this energy range should be above 10^8/s cm^2 or a current density of 10 pA/cm^2. This criterion for charging is useful for those concerned with predicting charging effects, particularly from the viewpoint of spacecraft safety.

The concept of a critical energy range has been noted by *Reagan et al.* [1981], who found that for SCATHA, the critical energy range was between 3 and 30 keV. This result remains valid in the context of the work shown here; the critical energy range has simply been narrowed.

The idea of a threshold dependence has been noted experimentally for ATS 5 and ATS 6, again by using the UCSD data sets, by *Garrett* [1981] (see his Figure 19). *Garrett* found that charging required an electron temperature of at least 2 keV (determined by integrating the distribution function and taking the ratios of the moments). The main difference in this study is in the identification of the critical energy range which causes the temperature to rise to a point where charging can begin. *Garrett et al.* [1980] have studied charging events for ATS 6 and correlated the spacecraft potential with particle fluxes in the 30- to 80-keV energy range. This differs slightly from the nature of the findings here, in that the threshold effect determines if the spacecraft will charge, not the magnitude of the charging. The same comment applies to distinguishing between the correlation established between 25-. to 75-keV energy electrons and charging by *Gussenhoven and Mullen* [1982]. One other distinction between this work and that of *Gussenhoven and Mullen* is that the correlation they show is for daylight charging, which involves different physical processes. Note also that their next lower channel, nominally from 11 to 35 keV, will probably sample electrons below the threshold energy, thus obscuring the importance of this energy range.

The threshold energy of 10 keV found here will vary from spacecraft to spacecraft, but the similarity of the responses by ATS 6 and SCATHA, which are vastly different spacecraft, suggests that any attempt to monitor the magnetosphere for charging prediction should include the 10- to 20-keV energy range.

Acknowledgments. The data presented here were provided by C. E. Mcllwain and analyzed under NASA contract NAS8-33982.

The editor thanks H. B. Garrett and J. B. Reagan for their assistance in evaluating this paper.

References

DeForest, S. E., Spacecraft charging at synchronous orbit, J. Geophys. Res., 77, 651-659, 1972.

Garrett, H. B., The charging of spacecraft surfaces, Rev. Geophys. Space Phys., 19, 577-616, 1981.

Garrett, H. B., and S. E. DeForest, Time-varying photoelectron flux effects on spacecraft potential at geosynchronous orbit, J. Geophys. Res., 84, 2083-2088, 1979.

Garrett, H. B., D. C. Schwank, P. R. Higbie, and D. N. Baker, Comparison between the 30- to 80-keV electron channels on ATS 6 and 1976-059A during conjunction and application to spacecraft charging prediction, J. Geophys. Res., 85, 1155-1162, 1980.

Greenspan, M. E., M. B. Silevitch, and E. C. Whipple, On the use of electron data to infer the structure of parallel electric fields, J. Geophys. Res., 86, 2175-2182, 1981.

Gussenhoven, M. S., and E. G. Mullen, A 'worst case' spacecraft charging environment as observed on SCATHA on 24 April 1979, paper presented at 20th Aerospace Sciences Meeting, Am. Inst. of Aeronaut. and Astronaut., Orlando, FL., 1982.

Kivelson, M. G., S. M. Kaye, and D. J. Southwood, The physics of plasma injection events, in Dynamics of the Magnetosphere, edited by S.-I. Akasofu, pp. 385-405, D. Reidel, Hingham, MA., 1979.

Knott, K., The equilibrium potential of a magnetospheric satellite in an eclipse situation, Planet. Space Sci., 20, 1137-1146, 1972.

Leung, M. S., M. B. Tueling, and E. R. Schnauss, Effects of secondary electron emission on charging, Spacecraft Charging Technology 1980, edited by N. J. Stevens and C. P. Pike, NASA Conf. Publ., 2182, 163-178, 1981.

Mauk, B. H., and C. E. Mcllwain, ATS 6 UCSD auroral particles experiment, IEEE Trans. Aerosp. Electron. Syst., AES-11, 1125-1130, 1975.

Mcllwain, C. E., Plasma convection in the vicinity of the geosynchronous orbit, in Earth's Magnetospheric Processes,

edited by B. M. McCormac, pp. 268-279, D. Reidel, Hingham, MA., 1972.

Olsen, R. C., The hidden ion population of the magnetosphere, J. Geophys. Res., 87, 3481-3488, 1982.

Olsen, R. C., C. E. Mcllwain, and E. C. Whipple, Observations of differential charging effects on ATS 6, J. Geophys. Res., 86, 6809-6819, 1981. Prokopenko, S. M. L., and J. G. Laframboise, Differential charging of geostationary spacecraft, J. Geophys. Res., 85, 4125-4131, 1980.

Reagan, J. B., R. W. Nightingale, E. E. Gaines, R. E. Meyerott, and W. L. Imhof, Role of energetic particles in charging/discharging of spacecraft dielectrics, Spacecraft Charging Technology 1980, edited by N. J. Stevens and C. P. Pike, NASA Conf. Publ., 2182, 74-85, 1981.

Rubin, A. G., P. L. Rothwell, and G. K. Yates, Reduction of spacecraft charging using highly emissive surface materials, in Proceedings of the 1978 Symposium on the Effects of the Ionosphere on Space and Terrestrial Systems, edited by John M. Goodman, pp. 313-316, Naval Research Laboratory, Washington, D. C., 1978.

Whipple, E. C., Jr., Observation of photo-electrons and secondary electrons reflected from a potential barrier in the vicinity of ATS 6, J. Geophys. Res., 81, 715-719, 1976.

Willis, R. F., and D. K. Skinner, Secondary electron emission yield behavior of polymers, Solid State Commun., 13, 685-688, 1973.

(Received May 5, 1982;
revised July 26, 1982;
accepted September 13, 1982.)